

Effective skyrmion number for mixed polarization states of light

Rosario Martínez-Herrero and Ángel S. Sanz

*Department of Optics, Faculty of Physical Sciences, Universidad Complutense de Madrid
Pza. Ciencias 1, Ciudad Universitaria – 28040 Madrid, Spain*

Polarization skyrmions are usually characterized through a unit Stokes vector field, which defines a map from the transverse plane to the Poincaré (Bloch) sphere and allows one to assign a skyrmion number under appropriate boundary conditions. This description assumes complete polarization. In many optical situations, however, the local polarization state is partially polarized and is therefore described by a spectral polarization matrix rather than by a single Jones vector. We formulate a density-matrix-based effective extension of the skyrmion-number construction for statistically stationary, quasi-monochromatic paraxial fields in terms of the normalized spectral polarization matrix. Its eigenvectors define two orthogonal polarization eigenstates, corresponding to antipodal points on the sphere, while the eigenvalue imbalance is fixed by the local degree of polarization $P(\mathbf{r})$. Averaging the opposite skyrmion-density contributions of these two eigenpolarizations leads to an effective skyrmion number in which the usual pure-state density is weighted by $P(\mathbf{r})$. The resulting quantity reduces to the conventional skyrmion number for fully polarized fields and vanishes in locally unpolarized regions. In general it is not an integer topological invariant; rather, it is an integrated effective measure, constructed from local Stokes parameters, of the skyrmionic content associated with the polarized part of a mixed optical field. We illustrate the construction with an analytic Gaussian-beam example in which a degree-one polarization texture is combined with a radially varying degree of polarization.

I. INTRODUCTION

Polarization textures provide a natural setting in which topology enters classical optics. When the local polarization state varies across the transverse plane, the associated Stokes vector may trace a nontrivial pattern on the Poincaré, or equivalently Bloch, sphere. In particular, polarization skyrmions are commonly described as maps from the transverse coordinate $\mathbf{r} = (x, y)$ to a unit vector on this sphere, with the corresponding skyrmion number measuring the signed wrapping of the sphere under suitable boundary conditions [1–5].

This construction is geometrically transparent, but it relies on an important assumption: the field is taken to be fully polarized at every point. Under this condition the local polarization state is represented by a Jones vector, or equivalently by a unit Stokes vector, and the usual skyrmion number is the degree of a map from the compactified transverse plane to the Poincaré sphere. The situation is less direct for partially polarized light. In that case the Stokes vector no longer lies on the surface of the sphere, but inside it, with a length given by the local degree of polarization (DoP). Thus the same optical field carries two distinct pieces of information: a polarization direction, when it is defined, and a local purity that quantifies how well defined that direction is.

Nonuniform partially polarized fields are not exceptional. They arise naturally from imperfect state preparation, incoherent superpositions, partial spatial or temporal coherence, scattering, or propagation through random or complex media. For such fields, a description in terms of a single Jones vector is insufficient. The standard object is instead the cross-spectral density matrix, and locally the spectral polarization matrix, which contains the second-order polarization information of a

statistically stationary, quasi-monochromatic field [6, 7]. After normalization, this matrix has the same structure as a two-level density matrix: its eigenvectors define two orthogonal polarization eigenstates, while its eigenvalues give their statistical weights.

This density-matrix structure provides a useful starting point for revisiting polarization skyrmions in mixed polarization states. At each point, the local polarization matrix can be viewed as an incoherent mixture of two antipodal pure polarization states on the Poincaré sphere. The imbalance between their weights is fixed by the DoP. Since the skyrmion density changes sign when the Bloch vector is inverted, the two eigenpolarization contributions do not add equally; their net contribution is controlled by this eigenvalue imbalance.

The central issue is therefore not whether a partially polarized field possesses an integer topological invariant of the same kind as a pure polarization texture. In general it does not. Rather, the relevant question is how to define a quantity that reduces to the usual skyrmion number in the fully polarized limit, gives no contribution from locally unpolarized regions, and remains expressed in terms of measurable polarization quantities. This is the point of departure for the effective skyrmion number considered below.

In this work we formulate such a quantity by taking the local spectral polarization matrix as the basic object. Section II reviews the mixed-state structure of this matrix and separates the eigentexture direction on the Poincaré sphere from the local DoP. Section III introduces the corresponding effective skyrmion number and relates the purity weighting to the spectral decomposition of the polarization matrix. Section IV applies the construction to an analytic Gaussian-beam example with a degree-one polarization texture and a radial DoP profile.

The conclusions are given in Sec. V.

II. POLARIZATION MATRIX AND MIXED-STATE STRUCTURE

We start from the standard local description of partially polarized paraxial fields. Consider a statistically stationary, quasi-monochromatic electromagnetic field whose transverse components are denoted by $E_i(\mathbf{r})$, with $\mathbf{r} = (x, y)$. Its second-order coherence and polarization properties are described by the cross-spectral density matrix

$$\hat{\mathbf{W}}_{ij}(\mathbf{r}_1, \mathbf{r}_2) = \langle E_i(\mathbf{r}_1) E_j^*(\mathbf{r}_2) \rangle, \quad (1)$$

where $\langle \bullet \rangle$ denotes an ensemble average. The local polarization state is obtained by evaluating the cross-spectral density matrix at coincident points,

$$\hat{\mathbf{J}}(\mathbf{r}) = \hat{\mathbf{W}}(\mathbf{r}, \mathbf{r}). \quad (2)$$

The matrix $\hat{\mathbf{J}}(\mathbf{r})$ is Hermitian and positive semidefinite. Its trace gives the local spectral density, whereas its normalized form contains the local polarization state. Different spatial-coherence properties may lead to the same local polarization matrix [8]; this does not affect the present construction, which is based only on local polarization information.

Using the Pauli matrices

$$\hat{\sigma}_1 = \begin{pmatrix} 0 & 1 \\ 1 & 0 \end{pmatrix}, \quad \hat{\sigma}_2 = \begin{pmatrix} 0 & -i \\ i & 0 \end{pmatrix}, \quad \hat{\sigma}_3 = \begin{pmatrix} 1 & 0 \\ 0 & -1 \end{pmatrix}, \quad (3)$$

together with $\hat{\sigma}_0 = \hat{\mathbf{I}}_2$, the spectral polarization matrix can be written in the Stokes representation [9–11] as

$$\hat{\mathbf{J}}(\mathbf{r}) = \frac{1}{2} \left[S_0(\mathbf{r}) \hat{\mathbf{I}}_2 + \sum_{j=1}^3 S_j(\mathbf{r}) \hat{\sigma}_j \right]. \quad (4)$$

Equivalently,

$$\hat{\mathbf{J}}(\mathbf{r}) = \frac{1}{2} \begin{pmatrix} S_0 + S_3 & S_1 - iS_2 \\ S_1 + iS_2 & S_0 - S_3 \end{pmatrix}, \quad (5)$$

where all Stokes parameters are evaluated at \mathbf{r} . With this convention, the scaled Stokes vector is

$$\mathbf{s}(\mathbf{r}) = \frac{1}{S_0(\mathbf{r})} (S_1(\mathbf{r}), S_2(\mathbf{r}), S_3(\mathbf{r})), \quad (6)$$

whose length corresponds to the local DoP,

$$P(\mathbf{r}) \equiv \|\mathbf{s}(\mathbf{r})\| = \frac{\sqrt{S_1^2(\mathbf{r}) + S_2^2(\mathbf{r}) + S_3^2(\mathbf{r})}}{S_0(\mathbf{r})}. \quad (7)$$

Thus $0 \leq P(\mathbf{r}) \leq 1$. A fully polarized state corresponds to $P(\mathbf{r}) = 1$, whereas $P(\mathbf{r}) = 0$ corresponds to a locally unpolarized state [6, 7].

The density-matrix structure becomes explicit after normalizing the polarization matrix by its trace,

$$\rho(\mathbf{r}) = \frac{\hat{\mathbf{J}}(\mathbf{r})}{S_0(\mathbf{r})}. \quad (8)$$

Since $\hat{\mathbf{J}}$ is Hermitian and positive semidefinite, it admits the spectral decomposition

$$\hat{\mathbf{J}}(\mathbf{r}) = \lambda_a(\mathbf{r}) |e_a(\mathbf{r})\rangle \langle e_a(\mathbf{r})| + \lambda_b(\mathbf{r}) |e_b(\mathbf{r})\rangle \langle e_b(\mathbf{r})|. \quad (9)$$

where $\lambda_a(\mathbf{r}) \geq \lambda_b(\mathbf{r}) \geq 0$ and the eigenvectors are orthonormal. The eigenvalues are fixed by S_0 and by the DoP,

$$\lambda_a(\mathbf{r}) = \frac{S_0(\mathbf{r})}{2} [1 + P(\mathbf{r})], \quad \lambda_b(\mathbf{r}) = \frac{S_0(\mathbf{r})}{2} [1 - P(\mathbf{r})]. \quad (10)$$

Thus partial polarization is locally equivalent to an incoherent mixture of two orthogonal fully polarized eigenstates, with an imbalance determined by $P(\mathbf{r})$.

For $P(\mathbf{r}) \neq 0$, the dominant eigenpolarization defines a direction on the Poincaré sphere. We parametrize the two eigenvectors as

$$|e_a\rangle = \begin{pmatrix} \cos(\theta/2) \\ e^{i\phi} \sin(\theta/2) \end{pmatrix}, \quad |e_b\rangle = \begin{pmatrix} -e^{-i\phi} \sin(\theta/2) \\ \cos(\theta/2) \end{pmatrix}. \quad (11)$$

which correspond to antipodal unit Bloch vectors $\pm \hat{\mathbf{n}}_0(\mathbf{r})$, with

$$\hat{\mathbf{n}}_0(\mathbf{r}) = (\sin \theta \cos \phi, \sin \theta \sin \phi, \cos \theta). \quad (12)$$

The normalized polarization matrix then takes the Bloch form

$$\hat{\rho}(\mathbf{r}) = \frac{1}{2} [P(\mathbf{r}) \hat{\mathbf{n}}_0(\mathbf{r}) \cdot \hat{\boldsymbol{\sigma}} + \hat{\mathbf{I}}_2]. \quad (13)$$

Equation (13) has the same form as the usual Bloch representation of a mixed two-level state, or qubit density matrix. In the present optical context, the corresponding Bloch sphere is identified with the Poincaré sphere of polarization states; we use the two terms interchangeably when referring to this geometric state space. It separates the two ingredients that will enter the topological construction below: the eigentexture $\hat{\mathbf{n}}_0(\mathbf{r})$, which gives the direction on the Poincaré sphere, and the DoP $P(\mathbf{r})$, which gives the local purity of the state. When $P = 1$, the state lies on the surface of the sphere and is fully polarized. When $0 < P < 1$, the direction remains defined by the eigenpolarization, but the Bloch vector has length P . At points where $P = 0$, the polarization direction is locally undefined.

Equivalently, the local state can also be written as a sum of a fully polarized component and an unpolarized background,

$$\hat{\mathbf{J}}(\mathbf{r}) = S_0(\mathbf{r}) P(\mathbf{r}) |E_p(\mathbf{r})\rangle \langle E_p(\mathbf{r})| + \frac{S_0(\mathbf{r})}{2} [1 - P(\mathbf{r})] \hat{\mathbf{I}}_2, \quad (14)$$

where $|E_p(\mathbf{r})\rangle$ is the pure polarization state. This form, which follows from the spectral decomposition theorem for positive definite matrices [10, 12], is to some extent analogous to Eq. (13), although in this case, physically, the first term carries the polarized part of the field, whereas the second term is locally unpolarized and carries no direction on the Poincaré sphere.

III. EFFECTIVE SKYRMION NUMBER FOR MIXED POLARIZATION STATES

For a fully polarized field, the local polarization state is represented by a unit vector $\hat{\mathbf{n}}_0(\mathbf{r})$ on the Poincaré sphere. If this vector field approaches a constant value at infinity, the transverse plane can be compactified to a sphere and $\hat{\mathbf{n}}_0(\mathbf{r})$ defines a map $S^2 \rightarrow S^2$. The corresponding skyrmion number (topological charge) is

$$N = \frac{1}{4\pi} \iint_{\mathbb{R}^2} \hat{\mathbf{n}}_0 \cdot (\partial_x \hat{\mathbf{n}}_0 \times \partial_y \hat{\mathbf{n}}_0) dx dy. \quad (15)$$

The integrand is the signed solid-angle density swept on the Poincaré sphere by an infinitesimal area element of the transverse plane. Under the above boundary condition, N is the degree of the map and is an integer topological invariant [2, 13, 14]. If the boundary condition is not satisfied, or if the integration is restricted to a finite observation window, Eq. (15) remains well defined but need not yield an integer [15].

For a partially polarized field, the normalized polarization matrix has the Bloch form given in Eq. (13). The local state is then represented by the Bloch vector

$$\mathbf{s}(\mathbf{r}) = P(\mathbf{r})\hat{\mathbf{n}}_0(\mathbf{r}), \quad (16)$$

whose length is the DoP. Thus the geometry of the eigentexture is still described by the unit vector $\hat{\mathbf{n}}_0(\mathbf{r})$, whereas the factor $P(\mathbf{r})$ measures how pure, or how well polarized, the local state is. In this case the state generally lies inside the Poincaré sphere and the integer topological interpretation of Eq. (15) is no longer available in terms of the mixed state itself.

The spectral decomposition of the local polarization matrix provides a density-matrix route to an effective density. The construction below should therefore be understood as a density-matrix-based effective quantity, not as a claim of a unique topological invariant for mixed polarization states. Let

$$\mu_a(\mathbf{r}) = \frac{\lambda_a(\mathbf{r})}{S_0(\mathbf{r})} = \frac{1+P(\mathbf{r})}{2}, \quad \mu_b(\mathbf{r}) = \frac{\lambda_b(\mathbf{r})}{S_0(\mathbf{r})} = \frac{1-P(\mathbf{r})}{2} \quad (17)$$

be the normalized eigenvalues. The two eigenpolarizations correspond to antipodal directions $\pm\hat{\mathbf{n}}_0(\mathbf{r})$ on the Poincaré sphere. For a pure texture, we denote the skyrmion number density (topological charge density) by

$$q(\hat{\mathbf{n}}_0) = \hat{\mathbf{n}}_0 \cdot (\partial_x \hat{\mathbf{n}}_0 \times \partial_y \hat{\mathbf{n}}_0). \quad (18)$$

Since this density changes sign under inversion of the Bloch vector, $q(-\hat{\mathbf{n}}_0) = -q(\hat{\mathbf{n}}_0)$, the density obtained by averaging over the two eigenpolarization contributions is

$$\begin{aligned} q_{\text{mix}}(\mathbf{r}) &= \mu_a(\mathbf{r})q(\hat{\mathbf{n}}_0) + \mu_b(\mathbf{r})q(-\hat{\mathbf{n}}_0) \\ &= [\mu_a(\mathbf{r}) - \mu_b(\mathbf{r})]q(\hat{\mathbf{n}}_0) \\ &= P(\mathbf{r})q(\hat{\mathbf{n}}_0). \end{aligned} \quad (19)$$

Thus the linear factor $P(\mathbf{r})$ follows from the local eigenvalue imbalance of the polarization matrix between the two antipodal pure-state contributions, which is also the length of the Bloch vector.

We therefore define the effective skyrmion number of a partially polarized field as

$$N_{\text{eff}} = \frac{1}{4\pi} \iint_{\mathbb{R}^2} P(\mathbf{r}) \hat{\mathbf{n}}_0 \cdot (\partial_x \hat{\mathbf{n}}_0 \times \partial_y \hat{\mathbf{n}}_0) dx dy. \quad (20)$$

All quantities entering Eq. (20) are determined by the local Stokes parameters, except at points where $P = 0$, where the polarization direction is undefined and the weighted contribution vanishes. This expression reduces to Eq. (15) in the fully polarized limit $P(\mathbf{r}) = 1$, and gives no contribution from locally unpolarized regions where $P(\mathbf{r}) = 0$. In general, however, N_{eff} is not an integer and should not be interpreted as a homotopy invariant. This distinction is important because mixed-state geometry can be treated in other, more formal ways, for example through interferometric mixed-state geometric phases or Uhlmann holonomy [16, 17]; the present construction is instead a local-polarization, Stokes-based effective measure. Specifically, it is an integrated effective measure obtained from the skyrmion density of the polarization eigentexture, with each local contribution weighted by the local DoP.

A useful limiting case is obtained when the DoP is uniform, $P(\mathbf{r}) = P_0$. Then Eq. (20) gives

$$N_{\text{eff}} = P_0 N. \quad (21)$$

Uniform depolarization therefore rescales the skyrmion number of the underlying eigentexture without modifying its geometry. For nonuniform $P(\mathbf{r})$, the effective number depends on the spatial overlap between the DoP and the local skyrmion density. This distinction will be illustrated in the analytic example below.

IV. ANALYTIC EXAMPLE: GAUSSIAN BEAM WITH A DEGREE-ONE TEXTURE

We now apply the definition of Eq. (20) to a cylindrically symmetric analytic model in which the polarization eigentexture is fixed and the DoP varies radially. The pure eigentexture has skyrmion number $N = 1$, so that any change in the effective number arises solely from the spatial weighting by the DoP. The particular profile chosen below is used only to obtain closed-form expressions; the definition in Eq. (20) does not rely on this choice.

A. Polarization matrix and eigentexture

Let (r, β) denote polar coordinates in the transverse plane, and consider a Gaussian intensity envelope

$$I(r) = I_0 \exp\left(-\frac{2r^2}{w_0^2}\right), \quad (22)$$

such that $S_0(\mathbf{r}) = I(r)$ in Eq. (14), and the pure state $|E_p\rangle$ is specified by the normalized Jones spinor

$$|E_p\rangle = \frac{1}{\sqrt{2(1+|\alpha|^2)}} \begin{pmatrix} 1 + \alpha \\ i(1 - \alpha) \end{pmatrix}. \quad (23)$$

with

$$\alpha(r, \beta) = \frac{\sqrt{2}r}{w_0} e^{i(\beta+\beta_0)} = \frac{r}{d} e^{i(\beta+\beta_0)}, \quad d = \frac{w_0}{\sqrt{2}}. \quad (24)$$

Here d sets the transverse scale of the polarization texture, and β_0 is a constant helicity angle. The corresponding unit Stokes vector is

$$\hat{\mathbf{n}}_0(r, \beta) = \left(\frac{2\xi \cos(\beta + \beta_0)}{1 + \xi^2}, \frac{2\xi \sin(\beta + \beta_0)}{1 + \xi^2}, -\frac{1 - \xi^2}{1 + \xi^2} \right), \quad (25)$$

with $\xi \equiv r/d$. As r increases from 0 to infinity, $\hat{\mathbf{n}}_0$ moves from the south pole to the north pole of the Poincaré sphere, while the azimuthal angle winds once around the beam axis. This is a representative degree-one stereographic texture used in discussions of paraxial optical skyrmions; the helicity β_0 rotates the in-plane texture without changing the skyrmion number [15, 18].

For the field described by Eq. (25), a direct calculation gives

$$q(\hat{\mathbf{n}}_0) = \frac{4}{d^2} \frac{1}{(1 + \xi^2)^2}. \quad (26)$$

Substitution into Eq. (15) yields $N = 1$, as expected for a degree-one texture.

B. DoP profile

To introduce partial polarization while preserving cylindrical symmetry, we choose the radial DoP profile

$$P_1(\mathbf{r}) = \frac{1 + \hat{n}_{0,3}(r)}{2} = \frac{\xi^2}{1 + \xi^2}, \quad (27)$$

where $\hat{n}_{0,3}$ is the third component of the unit Stokes vector (25). Thus, in this particular example, the DoP depends only on the latitude of the associated point on the Poincaré sphere.

The DoP profile (27) vanishes at the beam center and approaches unity for $r \gg d$ (or, equivalently, for $\xi \rightarrow \infty$). It therefore describes a situation in which the central region is dominated by the unpolarized contribution in

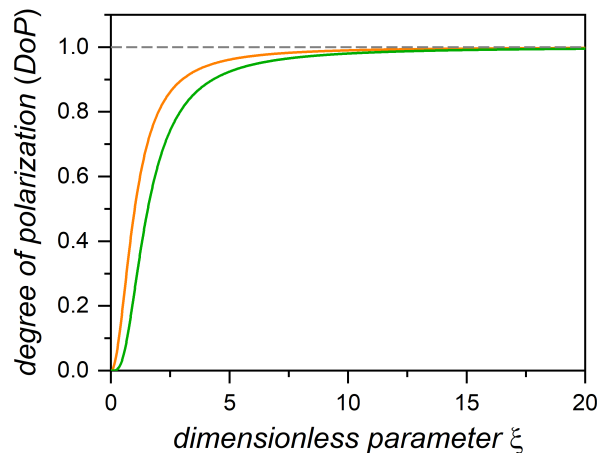


FIG. 1. Radial DoP profiles, $P_1(r)$ (orange solid line) and $P_2(r)$ (green solid line), used in the analytic example. Both increase monotonically from $P(0) = 0$, corresponding to a locally unpolarized state, to $P(\infty) = 1$, corresponding to the fully polarized limit. The horizontal (gray) dashed line marks $P(r) = 1$.

Eq. (14), while the outer region becomes essentially polarized. The choice is not unique, but it provides a simple analytic model in which the scale of the polarization texture and the scale of the purity variation are the same. The profile is shown in Fig. 1. For comparison, we also consider a second radial DoP profile,

$$P_2(\mathbf{r}) = \left(\frac{\xi^2}{1 + \xi^2} \right)^2, \quad (28)$$

which has the same limiting values as $P_1(r)$ but approaches unity more slowly (see Fig. 1).

C. Effective skyrmion number

Using Eq. (26), the effective skyrmion number associated with a general radial DoP profile (weight) $P(\mathbf{r})$ can be written as

$$\begin{aligned} N_{\text{eff}} &= \frac{1}{4\pi} \int_0^{2\pi} d\beta \int_0^\infty dr r P(r) \frac{4d^2}{(r^2 + d^2)^2} \\ &= 2 \int_0^\infty P(\xi) \frac{\xi}{(1 + \xi^2)^2} d\xi. \end{aligned} \quad (29)$$

For the profile in Eq. (27), this gives

$$N_{\text{eff},1} = 2 \int_0^\infty \frac{\xi^3}{(1 + \xi^2)^3} d\xi = \frac{1}{2}, \quad (30)$$

in terms of the dimensionless parameter ξ , while for the profile (28), we obtain

$$N_{\text{eff},2} = 2 \int_0^\infty \frac{\xi^5}{(1 + \xi^2)^4} d\xi = \frac{1}{3}. \quad (31)$$

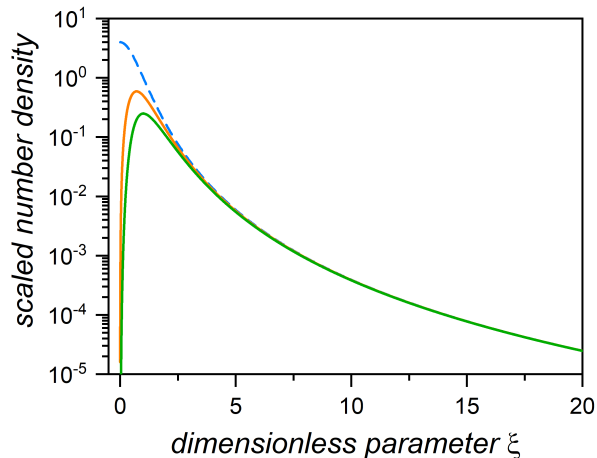


FIG. 2. Scaled skyrmion number density (blue solid line) and weighted number densities with $P_1(\mathbf{r})$ (orange solid line) and $P_2(\mathbf{r})$ (green solid line).

This second value serves as a diagnostic comparison: a DoP profile that remains below $P_1(\mathbf{r})$ over the relevant radial range produces a stronger suppression of the weighted skyrmion density and hence a smaller effective number.

Figure 2 compares the pure skyrmion density with its $P_1(\mathbf{r})$ - and $P_2(\mathbf{r})$ -weighted versions. The weight $P_1(\mathbf{r})$ suppresses the contribution from the central region, where the field is weakly polarized, without modifying the underlying eigentexture $\hat{\mathbf{n}}_0$. Yet $P_2(\mathbf{r})$ produces an even stronger suppression, as mentioned above.

The skyrmion number as a cumulative radial integral is shown in Fig. 3 for the three cases considered in Fig. 2. The pure skyrmion number approaches unity (blue dashed line), while the $P_1(\mathbf{r})$ -weighted effective number approaches $1/2$ (orange dashed line). The $P_2(\mathbf{r})$ -weighted curve approaches $1/3$ (green dashed line), illustrating again how slight differences between DoP's may lead to further reductions in the contribution from partially polarized regions.

This example separates the topology of the eigentexture from the purity of the local polarization state. The vector field $\hat{\mathbf{n}}_0$ remains a degree-one skyrmion, but the effective skyrmion number is reduced because the regions contributing to the skyrmion density are not equally polarized. In this sense, the noninteger value of N_{eff} reflects the spatial weighting of a fixed skyrmion density by the local DoP, rather than a change in the winding of the eigentexture itself.

V. CONCLUSIONS

We have examined how the skyrmion-number construction for polarization textures can be extended to optical fields whose local polarization state is mixed. The starting point is the spectral polarization matrix, which

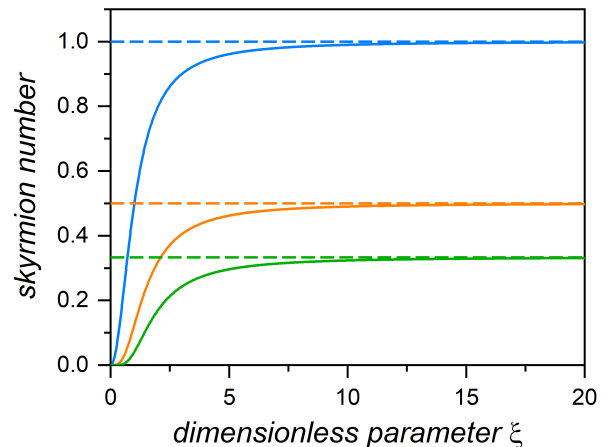


FIG. 3. Radial convergence (cumulative value) of the integrated skyrmion numbers: $N(r)$ (blue solid line), $N_{\text{eff},1}(r)$ (orange solid line), and $N_{\text{eff},2}(r)$ (green solid line). The horizontal dashed lines denote the corresponding asymptotic values, namely 1 , $1/2$, and $1/3$, respectively.

provides the appropriate local description of a statistically stationary, quasi-monochromatic partially polarized field. After normalization, this matrix has the form of a two-level density matrix: its eigenvectors define two orthogonal polarization eigenstates, associated with antipodal directions on the Poincaré sphere, and its eigenvalue imbalance is fixed by the local DoP.

This suggests that, in the context of partially polarized light or, in other words, mixed polarization states, we can define an effective skyrmion number in which the skyrmion density of the eigentexture is weighted by the local DoP $P(\mathbf{r})$. The weighting is not introduced as an independent assumption. It follows from averaging the skyrmion densities of the two antipodal eigenpolarizations, whose contributions have opposite sign and unequal weights. The resulting expression reduces to the conventional skyrmion number for fully polarized fields and gives no contribution from locally unpolarized regions.

The effective number is generally not an integer and therefore should not be interpreted as a homotopy invariant of the mixed state. Its role is more limited, but also more directly tied to measurable polarization quantities: it quantifies the skyrmion density of the underlying polarization eigentexture as weighted by the local polarized fraction of the field. In this sense, it separates the geometry of the eigentexture from the purity of the local polarization state.

The analytic Gaussian example makes this separation explicit. The chosen eigentexture has the pure-state skyrmion number $N = 1$, while the radial DoP profile reduces the effective value to $N_{\text{eff},1} = 1/2$. A second, more slowly increasing DoP profile, $P_2 = P_1^2$, gives $N_{\text{eff},2} = 1/3$, showing how reduced local polarization further suppresses the effective number. These values do not indicate a change in the winding of the eigentex-

ture; rather, they reflect the spatial overlap between the skyrmion density and the chosen DoP profile.

reconstructed locally.

ACKNOWLEDGMENTS

The formulation presented here is therefore best viewed as a density-matrix-based assignment of effective skyrmion content to partially polarized optical fields. The formulation applies directly to fields characterized by spatially resolved Stokes measurements, from which both $P(\mathbf{r})$ and the eigentexture direction $\hat{\mathbf{n}}_0(\mathbf{r})$ can be

The authors acknowledge financial support from the European Union NextGenerationEU/PRTR and MCIN/AEI/10.13039/501100011033 Project references PID2022-136796OB-I00 (R.M.-H.), PID2022-137569NBC42 (R.M.-H.), and PID2021-127781NB-I00 (A.S.S.).

-
- [1] S. Gao, F. C. Speirits, F. Castellucci, S. Franke-Arnold, S. M. Barnett, and J. B. Götte, Paraxial skyrmionic beams, *Phys. Rev. A* **102**, 053513 (2020).
 - [2] A. McWilliam, C. M. Cisowski, Z. Ye, F. C. Speirits, J. B. Götte, S. M. Barnett, and S. Franke-Arnold, Topological approach of characterizing optical skyrmions and multi-skyrmions, *Laser Photon. Rev.* **17**, 2300155 (2023).
 - [3] Y. Shen, Q. Zhang, P. Shi, L. Du, X. Yuan, and A. V. Zayats, Optical skyrmions and other topological quasiparticles of light, *Nat. Photon.* **18**, 15 (2024).
 - [4] C. Cheng, L. Rao, J. Ye, X. Zhao, Z. Che, W. Liu, J. Wang, and L. Shi, Navigating optical skyrmions—from historical origins to applications: tutorial, *Adv. Opt. Photon.* **18**, 1 (2026).
 - [5] C. Peters, N. Mata-Cervera, P. Ornelas, R. Warmbier, Y. Shen, and A. Forbes, Extracting topological features of skyrmionic light: a tutorial, *Adv. Photon.* **8**, 023001 (2026).
 - [6] L. Mandel and E. Wolf, *Optical Coherence and Quantum Optics* (Cambridge University Press, Cambridge, 1995).
 - [7] E. Wolf, *Introduction to the Theory of Coherence and Polarization of Light* (Cambridge University Press, Cambridge, 2007).
 - [8] R. Martínez-Herrero and P. M. Mejías, Relation between degrees of coherence for electromagnetic fields, *Opt. Lett.* **32**, 1504 (2007).
 - [9] R. W. Schmieder, Stokes-algebra formalism, *J. Opt. Soc. Am.* **59**, 297 (1969).
 - [10] C. Brosseau, *Fundamentals of Polarized Light: A Statistical Optics Approach* (John Wiley & Sons, New York, 1998).
 - [11] R. Martínez-Herrero, P. M. Mejías, and G. Piquero, *Characterization of Partially Polarized Light Fields* (Springer, Heidelberg, 2009).
 - [12] F. A. Graybill, *Matrices with Applications in Statistics* (Wadsworth, Belmont, CA, 1983).
 - [13] J. H. Han, *Skyrmions in Condensed Matter* (Springer, Cham, Switzerland, 2017).
 - [14] A. A. Belavin and A. M. Polyakov, Metastable states of two-dimensional isotropic ferromagnets, *JETP Lett.* **22**, 245 (1975).
 - [15] Z. Ye, S. M. Barnett, S. Franke-Arnold, J. B. Götte, A. McWilliam, F. C. Speirits, and C. M. Cisowski, Theory of paraxial optical skyrmions, *Proc. R. Soc. A* **480**, 20240109 (2024).
 - [16] E. Sjöqvist, A. K. Pati, A. Ekert, J. S. Anandan, M. Ericsson, D. K. L. Oi, and V. Vedral, Geometric phases for mixed states in interferometry, *Phys. Rev. Lett.* **85**, 2845 (2000).
 - [17] A. Uhlmann, Parallel transport and “quantum holonomy” along density operators, *Rep. Math. Phys.* **24**, 229 (1986).
 - [18] C. Cisowski, C. Ross, and S. Franke-Arnold, Building paraxial optical skyrmions using rational maps, *Adv. Photon. Res.* **4**, 2200350 (2023).